

# **Detection of Failed Conveyor Rollers Using an Acoustic Imager**

Remi Hart (1, 2), Antonio Morais (2), Dave Matthews (1), Jie Pan (1)

(1) The University of Western Australia (2) Alcoa Australia

#### **ABSTRACT**

Conveyors are widely used in the mining and resources industry and are critical to the efficient operation of many facilities. Inspecting these conveyors, particularly for failed rollers, is a major task, with some sites dedicating entire maintenance teams to the process. A key challenge in automating conveyor inspection is the reliable detection of failed rollers. This study investigates the use of an acoustic imager for roller fault detection and proposes a novel detection method. Controlled testing was conducted in an anechoic chamber on both new and failed rollers to examine limitations associated with source localisation, multiple sound sources, frequency ranges, and the directivity of roller noise emissions. The method was subsequently trialled on a trough conveyor at a resource facility stacking area and benchmarked against conventional inspection techniques. Results demonstrated enhanced detection sensitivity, with roller failures identified approximately 2.5 weeks earlier than by traditional methods.

#### 1 INTRODUCTION

Conveyors are a common piece of equipment within the mining and resources industry and are critical to the successful operation of many plants. They are typically constructed from standardized modules such as the example shown in Figure 1, each containing numerous idler rollers used to support the belt. Any breakdown of these conveyors may cost millions of dollars per day. Consequently, idlers must be inspected regularly for failure, a time consuming and challenging task. Once a failure is detected, the roller is replaced in either a planned or unplanned manner depending on severity. Planned replacement is preferred due to both efficiency [1, 2] and the safety [3] benefits.

The Pinjarra Alumina Refinery and Huntly Mine, located approximately 90 km south of Perth, operate more than 45 km of conveyors containing over 100,000 rollers. At both sites, roller inspection remains predominantly a manual process [4], requiring several hours of work each week. Despite this effort, manual inspections often fail to detect failures early enough to align with the 6-week planning cycle, leading to many rollers being replaced in an unplanned manner after final failure.

The significance of this issue is further highlighted by the emergence of automated systems capable of traversing conveyors with instrumentation to perform roller inspections. These systems are available in several configurations—including driverless vehicles, wheeled and tracked platforms, legged robots, and rail-mounted systems—each with specific advantages. While all are capable of carrying diverse payload instrumentation, their effectiveness in roller inspection is currently limited by the availability of suitable sensors.

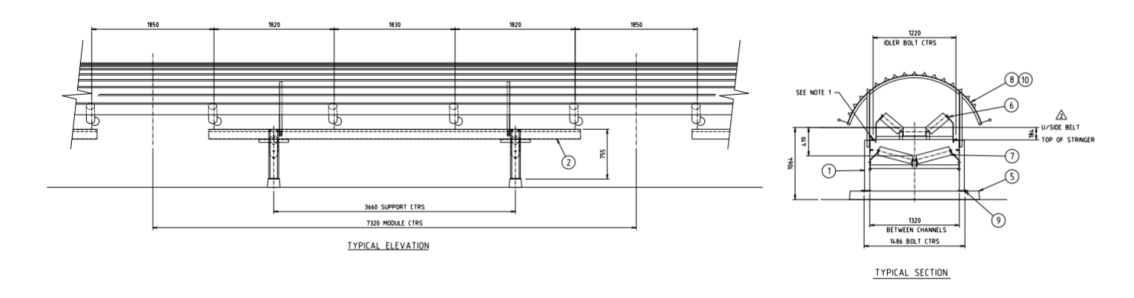


Figure 1: Drawing of a typical conveyor module.

ACOUSTICS 2025 Page 1 of 10

Due to the critical importance of roller inspection in the resources industry, significant work has been undertaken on failure detection in conveyor rollers. Most of this work falls into one of three main categories: thermal systems, non-directional acoustic systems, and embedded sensing systems. For this study, acoustic imaging method is used to measure noise emission from rollers. Acoustic imagers utilize an array of microphones to collect multiple streams of acoustic data. Following this, beamforming algorithms can be used to obtain the signal in different directions relative to the microphone array, forming an acoustic image. The use of acoustic imagers is now common practice for leak detection [5-7], even in high background noise environments. At the Pinjarra Refinery, a Fluke ii900 Acoustic Imager [8] is used for detection of both air and steam leaks, even in the high background noise environments presented within the plant. There has been some research into the application of acoustic cameras to conveyor systems. At present, this is primarily focused on noise source identification, targeting the reduction of noise emission. [9] proposed using an acoustic imager, to identify sources, and demonstrated potential in identifying the general area of sources using a 3.4 m diameter array. Following this, [10] has demonstrated lab testing with the intent of verifying correct operation of individual components. This lab testing showed promising results, however, is limited in applicability due to the lack of background noise in a laboratory environment when compared to that of a resources facility. To further add to this, [10] notes that their current method lacks analysis process automation, limiting its present usefulness.

An acoustic imager works by conducting beamforming. This is achieved through constructing a linear combination of the signal received by all microphones within the array. [11] this allows for the direction of sensitivity to be digitally varied through a range of angles, producing an image. Other methods of conducting this beamforming such as deconvolution are also used, although limited in use due to the increased processing intensity required. [12] However, all methods rely on uncombining the summed signals received by the microphones. Due to the summation of signals received, it is possible for 2 sources of the same frequency to appear as one source provided they are sufficiently close together. This resulting ambiguity of source location is a resolution limitation on the imager. [13]. This imager resolution has a number of components, notably, source frequency, microphone spacing, phase angle between the sources, and source spacing. [12]. This potential for resolution issues is a potential problem, with an example of merging of nearby sources shown in Figure 2.

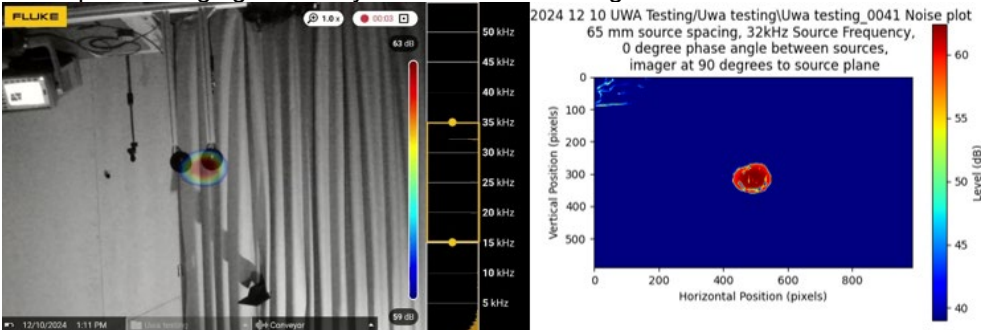


Figure 2: An acoustic image of test apparatus and corresponding noise plot showing source combination.

Both speakers are active at 32 kHz

### 2 OBJECTIVES

Objectives for this study are split into two main parts:

- 1. Determine the suitability of acoustic imaging as a conveyor roller inspection tool in an industrial setting.
- 2. Develop a metric for remaining useful life estimation for conveyor rollers based on acoustic imager data.

Within objective 1, there is a particular focus towards addressing the limitations of other inspection methods, primarily around detection resolution, detection time before failure, and deployment practicality. Within objective two, one of the key constraints is to ensure this is practical for full scale implementation. In order to satisfy this, the method proposed must be suitable for use on site, particularly considering who the current personnel conducting conveyor inspections are. As a result of this, there are two key resultant requirements:

- (1) Data processing should be mostly automated. This is to enable relatively unskilled operators to collect the required data and enables a move towards full inspection automation.
- (2) The imaging device should be robust, portable, and readily available. This is to enable the inspection to occur easily, and ease of widespread adoption of hardware.

To achieve this, data collection has been done using Pinjarra Refinery's Fluke ii900 imager. This device presents a manageable form factor, integrated data storage, and robust menus. This therefore enables ease of future deployment to maintenance teams with limited re-work.

Page 2 of 10 ACOUSTICS 2025

# 3 EXPERIMENTAL METHODS

#### 3.1 Imager Selection

A Fluke ii900 was arbitrarily selected as the test imager for this work. This handheld device employs a 64-microphone sunflower array and was chosen primarily for its availability.

# 3.2 Roller Data Extraction

Roller data from routine inspections using the Fluke imager was collected weekly over a 7-week period on a conveyor belt in Pinjarra Refinery's stacking area. In parallel, the operations and maintenance teams responsible for conventional conveyor inspections continued their work, with failures detected by these teams also recorded for comparison with the imager data. While full roller failures would have provided more complete data on the progression to final failure, many rollers are replaced beforehand to align conveyor downtime with other plant activities. As a result, detection by conventional methods was used as the comparison benchmark due to its availability and consistency across all rollers considered failed.

To preserve the validity of the comparison, the maintenance and operations teams were not provided with any information collected by the imager, nor with the full scope of the inspections—only that testing would occur on the scheduled day. This information was necessary to ensure safe access to plant areas and to minimize risks posed by multiple workgroups operating in the same location.

To collect the specific roller data, an inspection of an acoustic video as the camera is walked along the belt has been used. This has been selected as it is reflective of a possible deployment method, and is a practical way to obtain acoustic imagery of each roller in a timely manner. Furthermore, the motion of the imager allows distinction to be made between the source itself and potential reflections from other sources as discussed in section 4.6.1. A simplified flow for the roller data extraction code is detailed in Figure 3.

# 3.2.1 Frequency range

When collecting roller data, the imager was set to a frequency range of 15–35 kHz. This range was empirically determined through trial and error in a high background-noise environment, typical of conditions that challenge other acoustic systems. Testing in the Milling area at Pinjarra Refinery showed that this range is low enough to limit signal loss from attenuation and to reduce the occurrence of 'ghost sources' caused by spatial aliasing, while still being high enough to provide adequate resolution and minimize interference from other major noise sources in the area.

# 3.2.2 Roller feature extraction

An image processing AI based on the YOLO11 [33] model has been trained on imager footage to detect and construct bounding boxes around both the rollers and their supporting frames. An example of these bounding boxes is shown in Figure 4. From there, the surface integral of sound pressure inside the box is numerically calculated to estimate the noise emission from the roller. In addition, the Signal-to-Noise Ratio (SNR) of the box vs the remaining image is calculated as per Equation (1) to provide distinction between high roller noise and high background noise. These features are saved per roller for each frame, to enable later aggregation and processing.

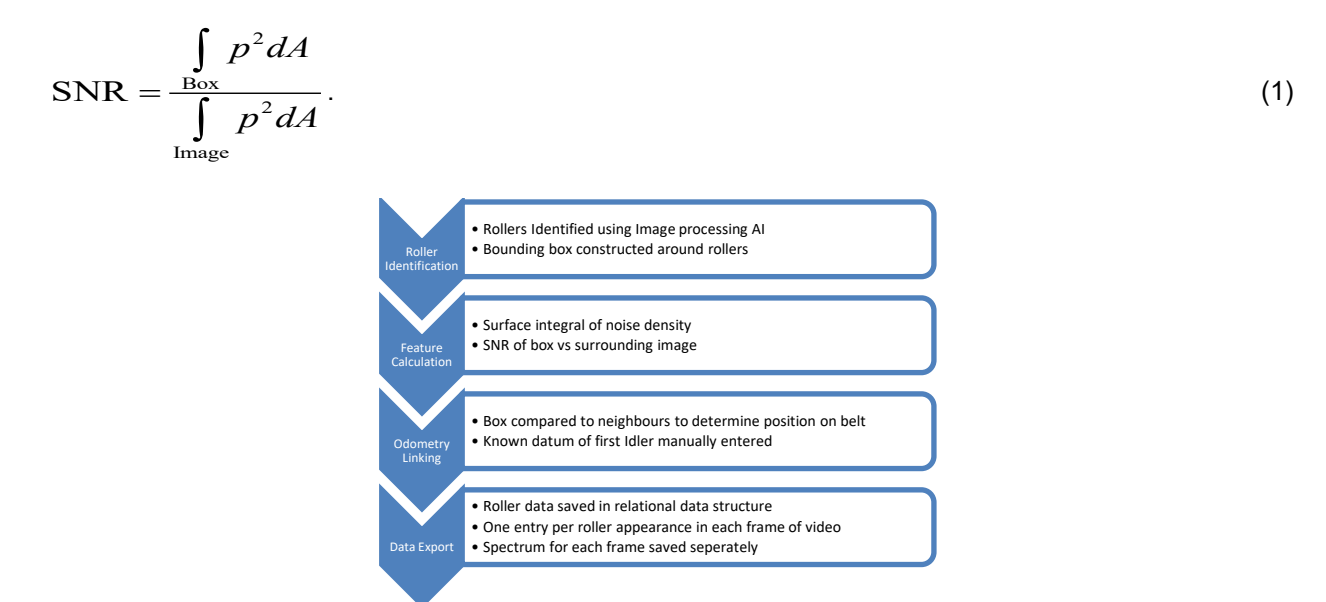


Figure 3: Simplified Flowchart for roller feature extraction

ACOUSTICS 2025 Page 3 of 10

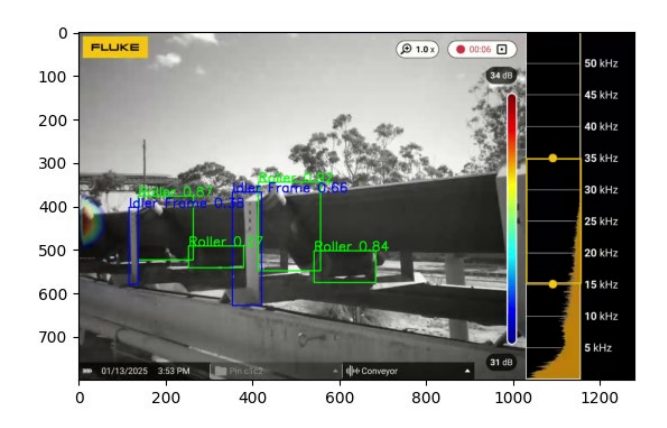


Figure 4: Sample Acoustic Image with Bounding Boxes around Objects

#### 3.2.3 Odometry

To identify which roller(s) along the belt are visible, a visual odometry system is used to track the imager's current view. Rollers are typically identified by the frame to which they belong, followed by their position within that frame. This identification system facilitates seamless integration with existing processes. First, supporting frames are labelled using the YOLO object tracking system. Each idler support frame is uniquely tracked throughout the video, and the frames are then indexed based on their order of appearance. The initial frame number is provided as an input parameter and saved by the user. Subsequently, rollers are iteratively linked to the frames based on their relative proximity as observed in the captured video.

#### 3.3 Roller Data Aggregation

For the final analysis, data for each roller is aggregated in a relational database. This database links the spectrum, roller, video metadata, and cepstra across multiple files, enabling long-term tracking and visualization of each roller's values over time. Within the database, the average power for each roller is calculated across all its appearances, along with the average SNR. Based on these metrics, the average noise level during a given measurement session is proposed as a failure indicator, while the average SNR serves as a measure of confidence that the observed noise level accurately reflects the roller's condition. A plot of these levels for some of the rollers is shown in Figure 5. As shown, some rollers are significantly higher in magnitude than others. These are the ones identified as likely to fail.

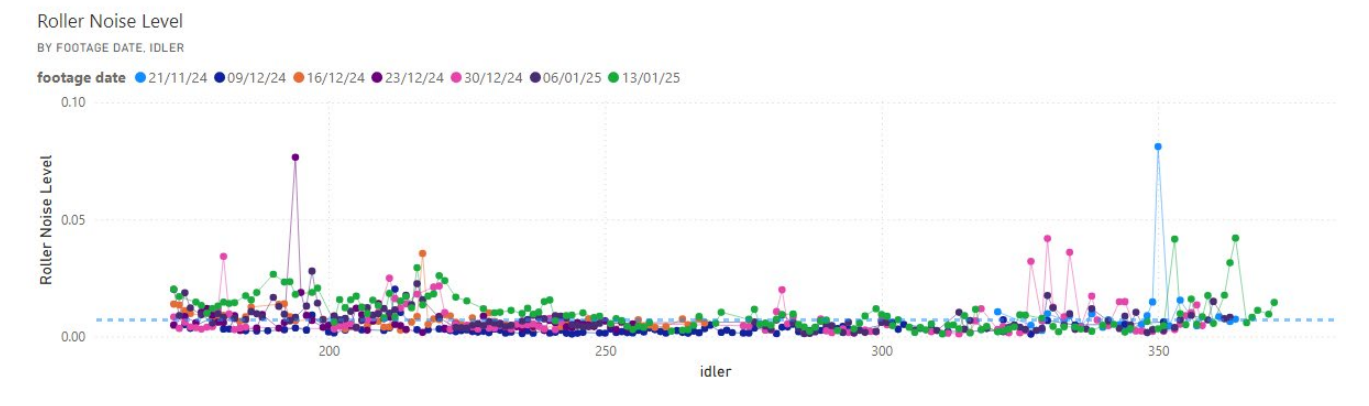


Figure 5: Observed Noise Levels for Rollers

In addition, these can be individually viewed to show failure progression over time, some examples of which are shown in Figure 6. As can be seen, this metric progresses towards failure of the rollers. In the case of these rollers, the site maintenance team applied failure tags in the interval between 06/01/2025 and 13/01/2025. This demonstrates the system's ability to indicate change over time, and the increased sensitivity offered by this method.

Page 4 of 10 ACOUSTICS 2025

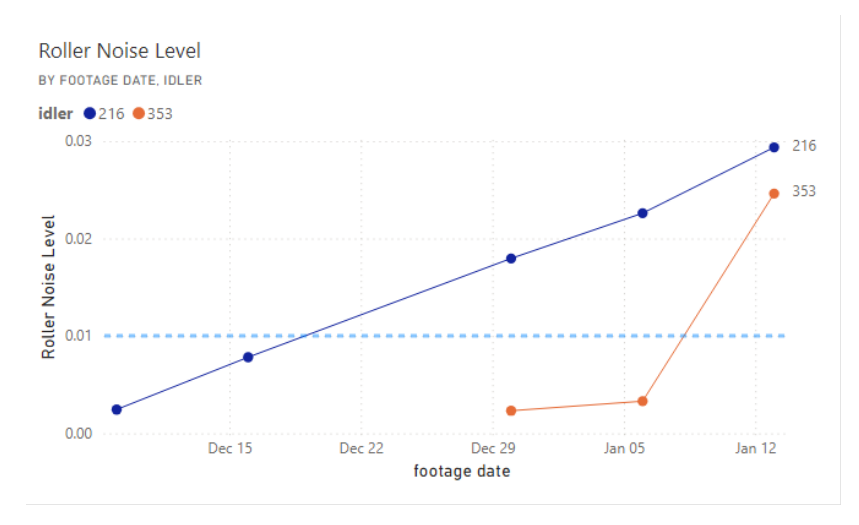


Figure 6: Failure progression of 2 rollers over time.

From these plots, a roller is deemed likely to fail when it is above a noise value of 0.01, with a SNR that is also above 0.04.

#### 3.4 Source Combination

As discussed in 2.2.2 there is the potential for source combination to occur if two sources of identical frequency have a small enough angular separation between them, particularly at lower frequencies. Anechoic chamber testing has been performed to determine the bounds over which this occurs for this particular imager and the frequency range of interest. The imager has been set up on a tripod pointing towards identical sources connected to a signal generator. As shown in Figure 7, the imager vertically aligned with the sources one meter away from the primary source to simulate an inspection. Testing has been conducted with the imager both perpendicular and at a 45-degree angle to the sources.

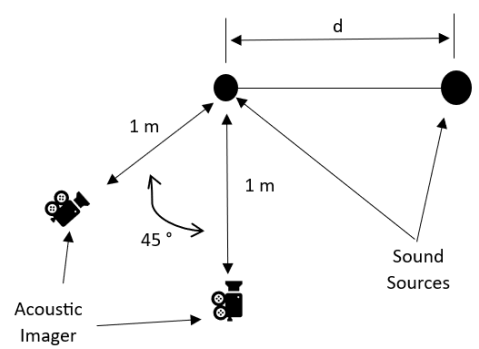


Figure 7: Test Setup for source Combination. d is varied from 65mm to 500mm

For both imager positions, a number of source-spacings have been tested, at a range of relative phase angles for the sources for both 16 and 32kHz source frequencies. Following this, the noise plots have been extracted from the acoustic video using the method discussed in section 4.2.2. A sample of these plots is shown in Figure 8. These plots were then qualitatively inspected for evidence of source combination, indicating that the imager has reached its resolution limits.

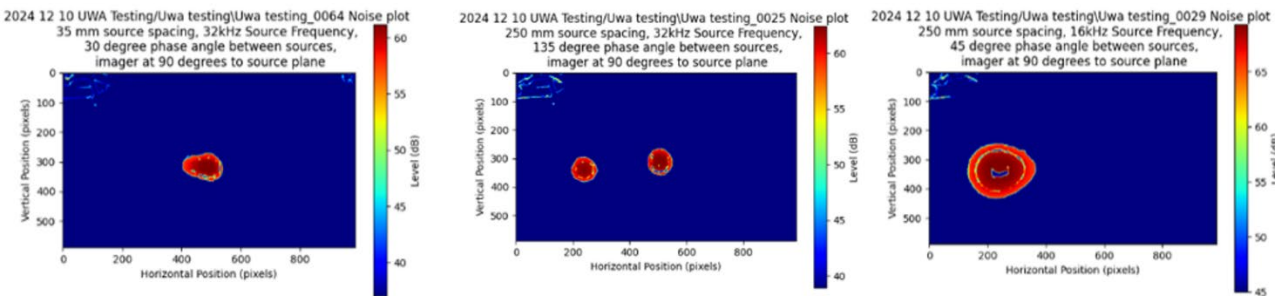


Figure 8: Example of source Combination

ACOUSTICS 2025 Page 5 of 10

# 3.5 Conventional Microphone Comparison

As part of testing, a comparative dataset was collected using a conventional condenser microphone for some of the rollers. This data was then compared with the spectrum exported from the imager to verify the microphone's behavior. The microphone data was acquired using a 192 kHz analog-to-digital converter, with the microphone positioned approximately 0.5 m from the roller under inspection. This was compared with data collected from the imager, which was held static for a short period to provide comparable measurements. To further support the comparison, background noise data for the conveyor was also collected while the conveyor was both online and offline, using a microphone placed 3 m from the conveyor.

#### 3.6 Other Considerations

In addition to the main considerations of source combinations and data acquisition, there are a few other phenomena of acoustic imaging worthy of noting, alongside with how the potential impacts of these phenomena have been addressed by the inspection and processing method discussed in sections 4.2 and 4.3.

#### 3.6.1 Reflections

Due to the high frequencies being used, it is accepted that reflection of sound off other environmental sources is possible. This has been empirically observed during testing as shown in Figure 9, confirming this behavior. Although reflections are present, the motion of the imager ensures they move relative to the reflecting surface as shown. As a result, these will only fall within the bounding box of the roller for some frames, and as such do not significantly contribute to the sound power levels being reported. In addition to the limited contribution to reported levels, the reflection will contribute to the noise used for calculating the SNR and as a result, an image with high reflections will be marked as low SNR, and therefore low reliability.

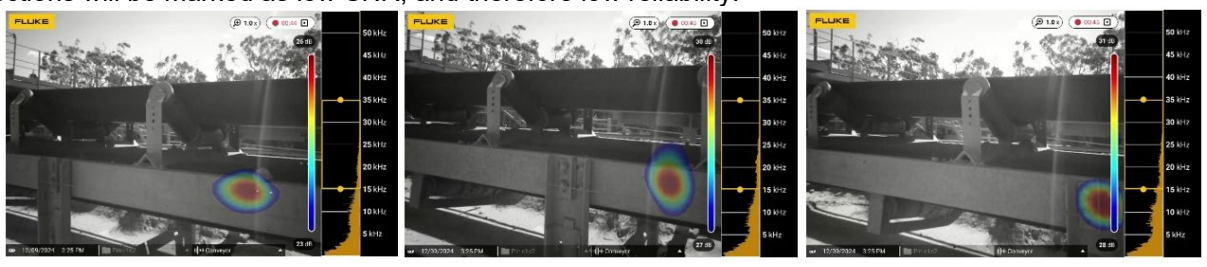


Figure 9: series of Acoustic images showing Motion of reflection relative to conveyor

# 3.6.2 Directivity of Emission

The directivity of a roller's acoustic emission may also have an impact on the detected signal. An estimation of this beampattern has been produced by collecting the emission level of a roller from multiple angles. These have then been plotted and interpolated to provide an approximation for the roller's emission pattern.

# 4 RESULTS AND DISCUSSION

# 4.1 Source Combination

From the plots in Figure 9, it is clear that there is the potential for source combination to occur in the interest range of the imager, typically occurring at a source spacing of 125 mm to 250 mm. This spacing for loss of resolution was dependent on frequency, occurring at 125 mm for 32 kHz and 250mm for 16 kHz. This result is less than the 330 mm length [34] of a roller, confirming that although source combination is possible, it will only occur for results within the one roller. As a result of this, sound coming from the center of rollers cannot be ignored, due to potential source combination. However, due to it requiring both sources to be within the length of one roller, it is unlikely that this impacts the overall results for an individual roller.

# 4.2 Conventional microphone comparison

The microphone data has been recorded and converted to a power spectrum for each roller. These can then be compared to both the background and the imager data. Figure 10 shows the frequency spectrum of the background noise at a few of these locations. Note that B1 is one of the other conveyors present in the area, while the numbers in the range 150-170 refer to the idler frame numbers along the belt. In the case of this data, roller 158 was performing appropriately whereas the roller in 166 was not and needed to be planned for replacement. The spectra shows that there is noticeable variation in background noise present in the environment. When recording the noise next to both a faulty and a non-faulty roller, these initially appear to be significantly similar, as shown in Figure 11. However, from Figure 12, it is evident that there is substantial difference in the roller noise once the background is subtracted, particularly in the 15-20 kHz range.

Page 6 of 10 ACOUSTICS 2025

In addition, it is noted that the considerable drop in level between 20 and 25 kHz is due to reaching the upper limit of this experimental setup's working frequency range.

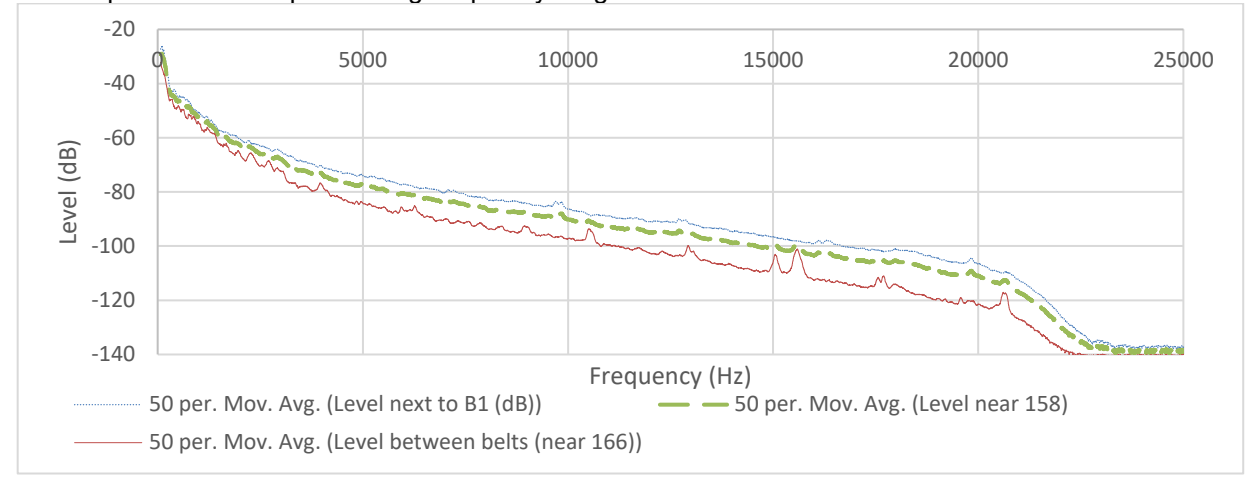


Figure 10: Background noise at various locations. Bracketed numbers refer to the numbered Idler frames along the belt's length

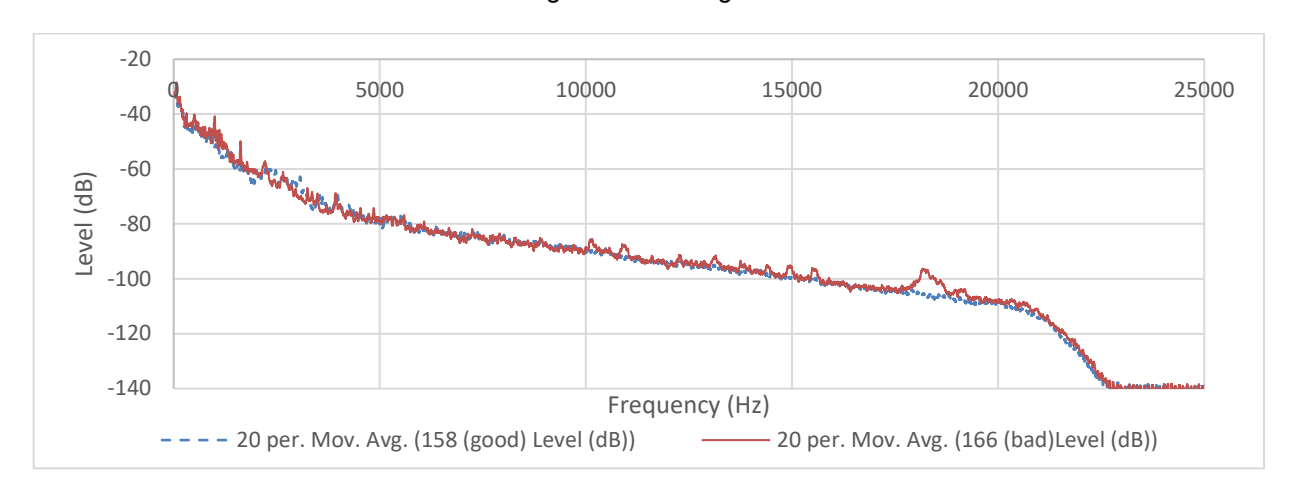


Figure 11: Noise near both a faulty and a non-faulty roller. Bracketed numbers refer to the numbered Idler frames along the belt's length

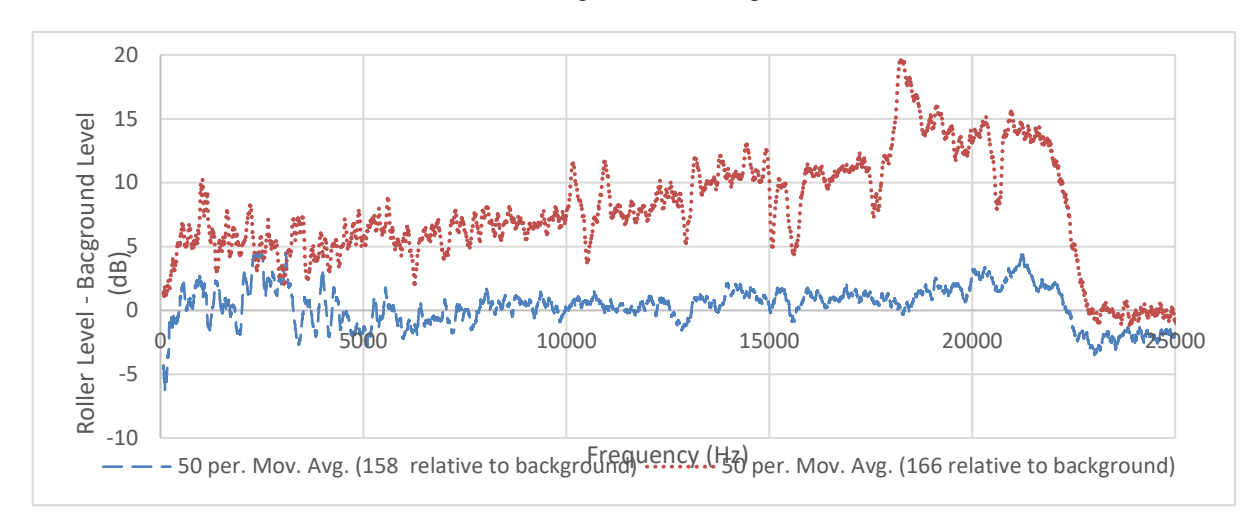


Figure 12: Roller noise relative to background. Bracketed numbers refer to the numbered Idler frames along the belt's length

ACOUSTICS 2025 Page 7 of 10

From looking at Figure 12 in detail it is also evident that the difference in amplitude exhibited by faulty rollers is particularly present in the 15-20kHz range, further confirming the selection of 15-35kHz as the target frequency range for the imager.

Comparing this data for specific rollers to that collected by the imager shows that the imager data is similar to that collected by the microphone as shown in Figure 13, with a sizeable gain applied. This is numerically confirmed, with a correlation coefficient of 0.95 between the imager and the microphone for the range of 2 to 20 kHz. The range of 2 to 20 kHz has been selected for this as 2 kHz is the rated minimum as specified by the imager manufacturer [27], while 20 kHz is approaching the limit of the microphone's frequency range.

# 4.3 Comparison With Manual Detection

Over the test duration, the location maintenance team identified 30 rollers on the test conveyor as likely to fail and requiring maintenance. In all cases, these have been identified in advance by the acoustic imager, with the distribution of detection time difference shown in Figure 14. This detection time difference between conventional methods and the proposed method had a mean of 2.6 weeks, with an estimated 95% confidence interval for the mean being [2.1345, 3.0655]. This shows a significant improvement in detection sensitivity and can be seen as a promising result for the use of acoustic imaging as an inspection method.

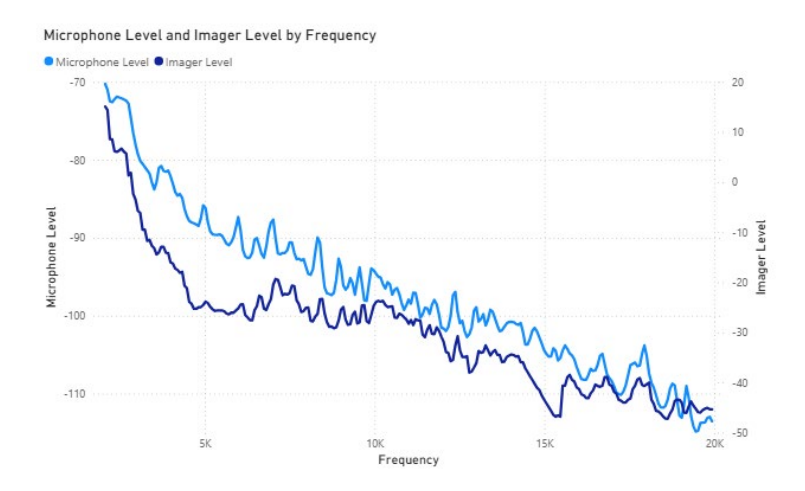


Figure 13: Comparison of Imager and microphone data

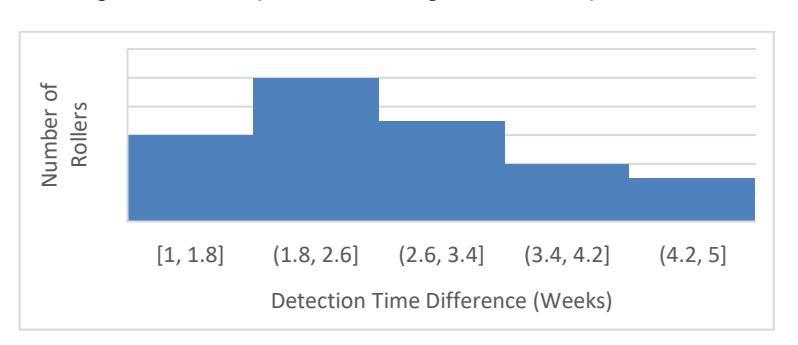


Figure 14: Histogram of the observed Difference in detection Time between Acoustic Imaging and conventional Methods

# 4.4 Emission Directionality

From the directional sound measurements, an estimation of the directionality field can be constructed and is presented in Figure 15. From this, it can be seen to be similar to the combination of a hollow cylinder plus a torus. This makes some sense, considering a roller shell as a hollow cylinder, and the bearings can be very loosely approximated as a torus. From the perspective of roller inspection, this is important to note as angle from which the roller is viewed will have a slight impact on the measured result. In the case of the proposed methodology, this is overcome by sweeping through a number of viewing angles and averaging the result. As a result of this averaging and the limited Emission change, it is not expected to have a significant impact on measured results.

Page 8 of 10 ACOUSTICS 2025

Proceedings of ACOUSTICS 2025 12-14 November 2025, Joondalup, Australia

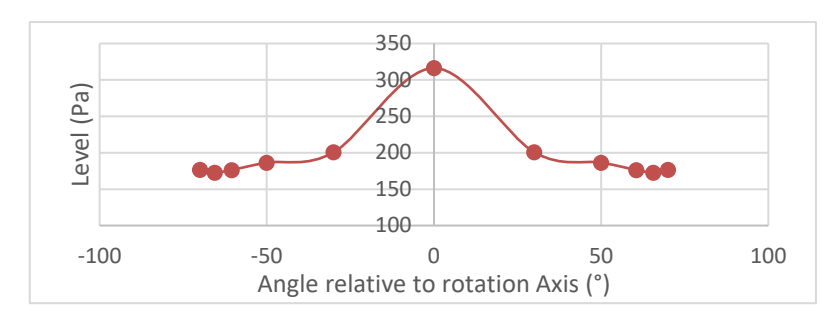


Figure 2: Observed Directionality of Roller Emission

# 4.5 Implications for Conveyor Inspection

These results show acoustic imaging is a potential method for automated conveyor roller inspection. This method provides an acoustic system, capable of identifying rollers at the individual level autonomously, in the form of commercially available hardware. This enables a significant reduction in maintenance resource consumption due to conveyor inspection.

# 5 CONCLUSIONS

This work presents a potential method for detecting conveyor roller failure using an acoustic imager. The results provide the directivity of the acoustic emission from a faulty roller, a correlation between data from the imager and a conventional microphone, and testing results on the resolution limits of the imager. Based on these findings, a method for identifying faulty rollers has been proposed and compared to conventional approaches, showing a performance improvement of approximately two weeks over the manual method.

# **ACKNOWLEDGEMENTS**

The authors gratefully acknowledge the support of the Pinjarra Alumina Refinery for providing access to both the imager and the conveyors used in this research.

# **REFERENCES**

- [1] J. Apps, "Reactive vs. Proactive Maintenance," vol. 2024, ed: ARMS Reliability, 2024.
- U. C. Group, "Planned Maintenance: Converting Unplanned Work to Increase Uptime," vol. 2024, ed: USC Consolting Group, 2020.
- [3] C. Dempsey, "Review of Significant Incidents to understand impact of planned/unplanned maintenance," School of Mechanical and Chemical Engineering, University of Western Australia, Perth, 2014.
- [4] T. Vergone, "Overland Conveyor Belt Patrol and Reporting," Alcoa Of Australia, 2023, AUACDS-2053-4977
- [5] "Visualizing Sound with the FLIR Si124: an Acoustic Imaging Camera." Teledyne FLIR. https://www.flir.com.au/discover/instruments/acoustic-imaging/visualizing-sound-with-the-flir-si124-acoustic-imaging-camera/ (accessed.
- [6] B. Schiricke, M. Diel, and B. Kölsch, "Field Testing of an Acoustic Method for Locating Air Leakages in Building Envelopes," *Buildings*, vol. 14, no. 4, p. 1159, 2024.
- [7] T. Senan, "Leak Rate Quantification (LRQ) Method for Acoustic Imaging Cameras," ed: Fluke, 2021.
- [8] "Fluke ii900 Industrial Acoustic Imager." Fluke. https://www.fluke.com/en-au/product/industrial-imaging/sonic-industrial-imager-ii900 (accessed 2024).
- [9] G. Fedorko, P. Liptai, and V. Molnár, "Proposal of the methodology for noise sources identification and analysis of continuous transport systems using an acoustic camera," *Engineering Failure Analysis*, vol. 83, pp. 30-46, 2018, doi: 10.1016/j.engfailanal.2017.09.011.
- [10] P. Bortnowski, A. Nowak-Szpak, M. Ozdoba, and R. Król, "The Acoustic Camera as a Tool to Identify Belt Conveyor Noises," *Journal of Sustainable Mining*, vol. 19, no. 4, pp. 286-294, 2021, doi: 10.46873/2300-3960.1036.
- [11] B. D. V. Veen and K. M. Buckley, "Beamforming: a versatile approach to spatial filtering," *IEEE ASSP Magazine*, vol. 5, no. 2, pp. 4-24, 1988, doi: 10.1109/53.665.
- [12] P. Chiariotti, M. Martarelli, and P. Castellini, "Acoustic beamforming for noise source localization Reviews, methodology and applications," *Mechanical Systems and Signal Processing*, vol. 120, pp. 422-448, 2019/04/01/ 2019, doi: https://doi.org/10.1016/j.ymssp.2018.09.019.
- [13] A. Cigada, M. Lurati, F. Ripamonti, and M. Vanali, "Beamforming method: Suppression of spatial aliasing using moving arrays," 01/01 2008.
- [14] Ultralytics YOLO11. (2024). [Online]. Available: https://github.com/ultralytics/ultralytics

ACOUSTICS 2025 Page 9 of 10

[15] R. M. Vergone, P, "ME400050-372," in *TROUGH IDLER ROLLER 915 X 40 DETAILS*, ed: ALCOA OF AUSTRALIA LIMITED, 1998.

Page 10 of 10 ACOUSTICS 2025